Development of the Slovak 70-cm Optical Passive System Dedicated to Space Debris Tracking on LEO to GEO orbits

J. Šilha, S. Krajčovič, M. Zigo, D. Žilková, P. Zigo, J. Šimon, J. Tóth and L. Kornoš

Faculty of Mathematics, Physics and Informatics, Comenius University in Bratislava, Slovakia

S. J. Setty

ESA/ESOC, Space Debris Office, Robert-Bosch-Strasse 5, DE-64293 Darmstadt, Germany

T. Flohrer

ESA/ESOC, Space Debris Office, Robert-Bosch-Strasse 5, DE-64293 Darmstadt, Germany

B. Jilete

Camino Bajo de Castillo S/N, 28692 Villanueva de la Canada, Madrid, Spain

ABSTRACT

The Faculty of Mathematics, Physics and Informatics of Comenius University in Bratislava, Slovakia (FMPI) has been developing its 70 cm Newtonian design telescope (AGO70) since 2016 within the framework of the ESA Plan for Cooperating States (PECS) programme for Slovakia. The ongoing development is performed for space debris tracking situated from Low Earth Orbit (LEO) to Geosynchronous Earth Orbit (GEO) and is focused on the improvement of hardware, system control software, image processing software and the observation program.

The AGO70 has been installed at the FMPI's Astronomical and Geophysical Observatory in Modra, Slovakia (AGO) in Fall 2016. It was a standard astronomical system capable to perform measurements of e.g. stellar objects, near Earth asteroids, comets, etc. To achieve that the system could be effectively used for space debris research and space surveillance tracking (SST), there were several predefined objectives to be accomplished. First, the hardware, e.g., telescope mount, needed to be evaluated quality-wise and improved. Secondly, it was imperative to adapt the low-level telescope control for the needs of space debris tracking. Thirdly, the image processing software has been developed in a modular way and validated. The observation planning has been formulated according to the AGO70 system's hardware limitations with focus on LEO, GTO, GNSS and GEO like orbits. To verify the system's capabilities, an observation campaign was performed.

In our work we present the AGO70 systems description and the requirements defined for the hardware, software and observation program to achieve the desired capabilities. We compare the system's performance before and after the improvements have been and will be implemented. Discussed are the space debris observation programs of the AGO70 system with focus on system's output data description, their quality and formats.

1. INTRODUCTION

1.1 Motivation

Continuous growth of the space debris population in Low Earth Orbit (hereafter LEO) region, orbits with mean altitudes above the Earth orbit below 2000 km, is posing instantaneous threat to the satellite infrastructure. The possibility to pollute the LEO region increases even more with so-called mega-constellations, constellations with hundreds to thousands of small satellites [1]. It is expected that a number of malfunctioning satellites will increase with the rising satellite population and these non-controlled objects will pose a risk to the environment [2]. At current stage the LEO surveys and cataloguing are performed mostly by the USSTRATCOM (United States Strategic Command) (hereafter public catalogue), which also provides free access to the data. These data for LEO objects are gathered mostly by performing radar observations, while for higher orbits the passive optical sensors (hereafter telescope) are used.

The new approach to perform the LEO object tracking and cataloguing is considered by the operators of the Satellite Laser Ranging (hereafter SLR) sensors (also known as active optical sensors) [3]. The recent development in space debris tracking with SLR sensors showed promising results [4], [5]. The existing, improved and new SLR sensors capable of LEO debris tracking can be used to maintain own LEO SLR catalogue as stated in [3]. The objects size limit for such tracking is questionable at this stage, but it is foreseen to reach the size limits comparable of the public catalogue (diameter above 10 cm).

Using telescope for LEO survey and tracking is in general more complicated than to use it for GEO population. LEO objects have considerably higher apparent angular rates, reaching few degrees per second. The object is visible only once illuminated by the sun while the observer is already in Earth's shadow. Therefore, the visibility windows are relatively short, only few hours after dusk and before dawn. For that reason, multiple sensors and sophisticated strategies are needed to make the surveys with optical passive sensors feasible [6].

To create a SLR LEO catalogue, as proposed in [3], there must be established connections between the survey systems or existing catalogues and the tracking systems. In our case we will be assuming the public catalogue maintained by the USSTRATCOM [7] as the source of data to be improved to certain level by telescope and then tracked by the SLR systems. Once the orbits are sufficiently accurate for the SLR sensors (object is visible in the FOV), the SLR network can take over the tracking.

1.2 AGO70 system

Slovakia became the 9^{th} ESA European Cooperative State in 2015. The Department of Astronomy and Astrophysics (DAA), Faculty of Mathematics, Physics and Informatics of Comenius University in Bratislava, Slovakia (FMPI) was granted resources from the first and third ESA PECS calls to action to transform a 0.7-m Newtonian telescope (hereafter AGO70) (see Fig. 1) used for amateur observations into a professional optical system capable of tracking space debris and other naturally formed objects. Another part of this activity is to develop a software (in coordination with the Department of Applied Informatics, FMPI) that would handle and process images yielded by the newly acquired telescope.

Fig. 1: AGO70 telescope in the small dome of the Astronomical and Geophysical Observatory in Modra, Slovakia (AGO).

The AGO70 system is on an equatorial mount and has a very thin 700 mm parabolic mirror from Alluna optics supported by gravity actuator. The focal length of the system is 2962.0 mm. System is equipped with a front-illuminated CCD FLI Proline PL1001 Grade 1 with a resolution of 1024 x 1024 pixels where a pixel size is 24 μm. This results in an effective field-of-view (FoV) of $28.5' \times 28.5'$ and iFOV of $1.67''/pixel$. A filter wheel containing the Johnson-Cousins BVRI filters is placed in front of the CCD.

2. OBSERVATIONS

2.1 Planning

Observation planning of AGO70 depends on the selected observation programs. Except one, all of them are dedicated to the space debris research. We perform astrometry of calibration objects such as Global Position System (GPS) satellites or GLONASS satellites. This observations help to validate the acquired data quality [8]. Astrometry is also acquired for the LEO objects which are observed to test the system timing and obtain test data for LEO astrometric analysis. Photometric measurements are acquired to achieve two different goals: obtain the information about the rotational state of the objects by analyzing the rotational light curves; obtain the surface characteristics of the object by using BVRI filters.

Planning itself is performed with FMPI's internal tool SatEph which is built on the SGP4 model [9]. The software uses the Two-Lines Elements (TLE) obtained from the public catalogue to calculate the exact position of the object for given observer and observation epoch. This tool allows user to select appropriate object, e.g. object with required angular velocity, and visualize its position compared to the telescope's pointing. SatEph provides to the user with the additional information such as elevation above the horizon, phase angle, observer-object range, etc. The Graphic User Interface (GUI) of SatEph program can be seen in Fig. 2.

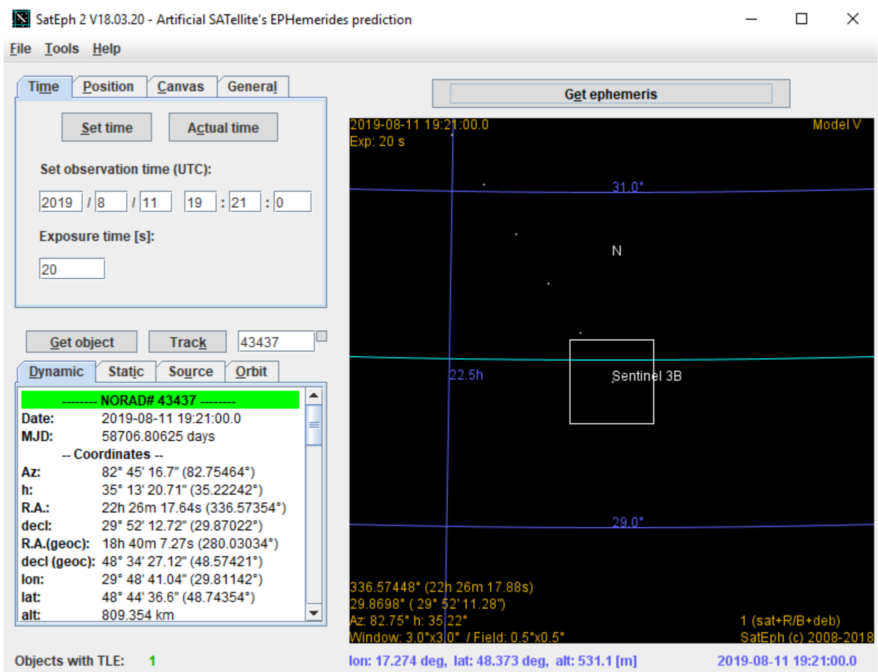

Fig. 2: Main GUI components of the FMPI's observation planning tool SatEph.

2.2 Data acquisition

Measuremets are acquired by using FMPI's internal tool Low-Level Telescope control (LLTC). This system is responsible for control of the CCD camera, mount, filter wheel and it reads actual pointing position from the encoders. The control PC's system time is synchronized with the internet and its accuracy is up to 80 ms [10].

The examples of FITS frames acquired by using four different observations strategies with the AGO70 system are shown in Fig. 3 and Fig. 4. The West direction is always to the right and the North is always upwards. Fig. 3 shows example for the series acquired for the AGO70 system validation and light curve extraction. Shown is frame composition containing four stacked images for GPS satellite 14068A (Fig. 3a) acquired by the AGO70 system in March 2018. For this GPS satellite we used sidereal tracking with the exposure time set to 0.1 s which led the stars and object to appear as points on the resulting frames. Fig. 3b shows example of light curve series acquisition by using the GEO tracking. Shown is the composition of frames, 87 in total, for the Delta 4 R/B (02051B) observed by the

AGO70 system in December 2018. In Fig. 4 depicts two frames for the LEO objects acquired during August 2019. In Fig. 4a shows a frame acquired for the ESA satellite Sentinel 3B (18039A). During the image acquisition we used sidereal tracking which led to the object to appear as a streak on the frame, while the stars appear as points. Fig. 4b shows a frame acquired for the upper stage SL-12 R/B(2) (02037D). During the image acquisition the object tracking was used which led to the object to appear as a point on the frame, while the stars appear as streaks. The observations times for the Fig. 3 and Fig. 4 are for the start of the exposure for the first frame in UTC.

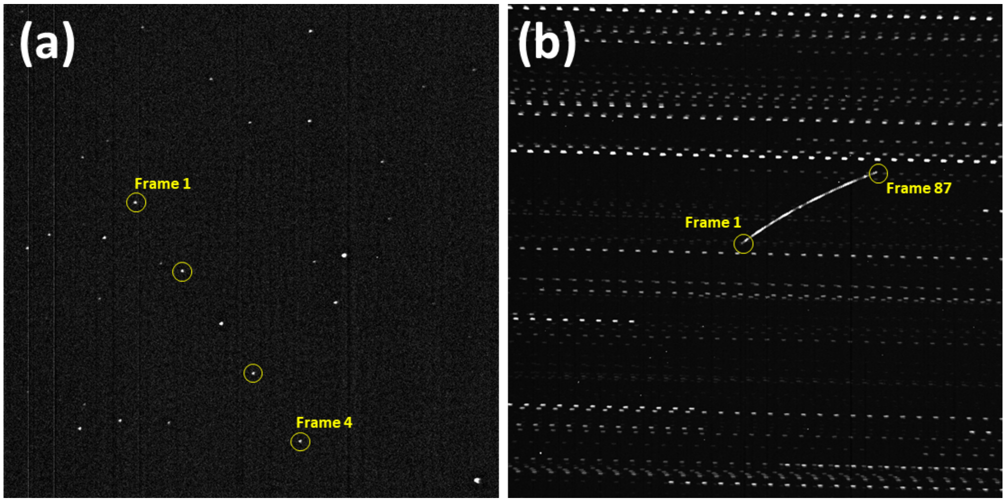

Fig. 3: Example of FITS series acquired by the AGO70 system for the GPS and GEO objects: (a) composition of 4 frames acquired for GPS satellite 14068A (exp = 0.1s, R filter, sidereal, 2018-03-22T01:00:57) by using the sidereal tracking; (b) composition of 87 frames acquired for Delta 4 R/B (02051B) (exp = 1.0s, R filter, GEO, 2018-12-05T04:28:47) by using the GEO tracking. Data were acquired for the AGO70 system's calibration/validation and light curve extraction, respectively.

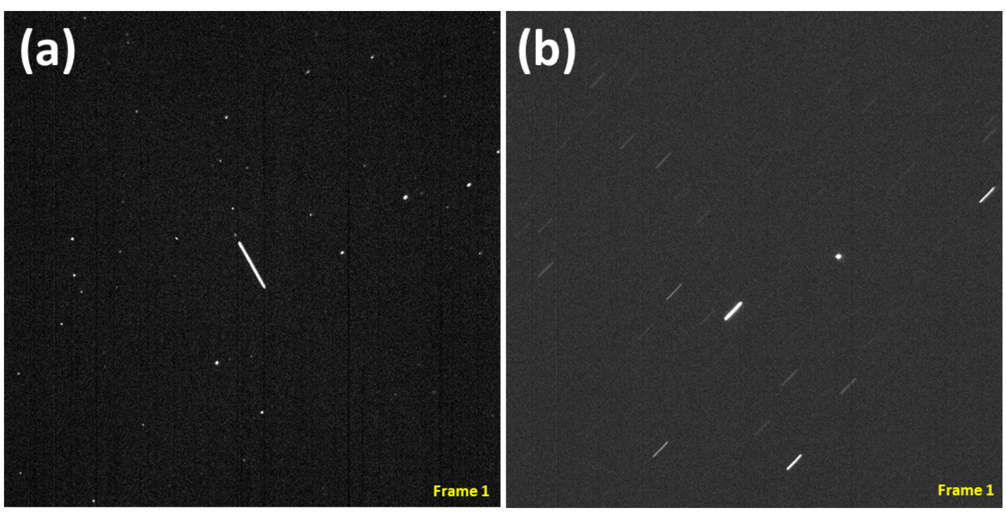

Fig. 4: Example of two FITS frames acquired by the AGO70 system for the LEO objects. (a) the FITS frame acquired for Sentinel 3B (18039A) (exp = 0.1s, R filter, 2019-08-11T19:21:00) by using the sidereal tracking; (b) the FITS frame acquired for SL-12 R/B(2) (02037D) (exp = 0.1s, I filter, '2019-08-27T19:55:24.5) by using the object tracking. Data were acquired for the AGO70 system's calibration/validation and IPS testing.

3. DATA PROCESSING

We distinguish two types of processing in our work: the conventional processing when we use typical astronomical tools such as Astrometrica [11] (see Section 3.1) and AstroImageJ (AIJ) (see Section 3.2) [12]; and the experimental processing when we use by us developed modular-based software suit Image Processing System (IPS) (see Section 3.3) which contains several different Image Processing Elements (IPE) [8].

3.1 Astrometry

Conventional astrometry is performed with Astrometrica software. This is a well-established tool in astronomical community. For satellites and debris objects on GEO it is necessary to choose a very short exposure time, 0.1 s - 0.2 s, to get objects and stars to appear as point like objects on the resulting frame (see Fig. 3a). This is independent on the tracking type (sidereal vs. GEO). This type of frames can be directly processed by Astrometrica.

Astrometry of objects on LEO orbits requires a more complicated approach. In this case the stars appear as points while object appears as a streak (see section Fig. 4a) or other way around (see Fig. 4b). These observations are focused on the astrometric data acquisition of LEO objects with a goal to improve their TLE. This type of frames require us to use IPS (see Section 3.3) rather than Astrometrica tool.

3.2 Light curves

Light curves are acquired during GEO tracking and the shortest used exposure time is 1.0 s. This usually leads to high Signal-to-Noise Ratio (SNR) for large compact object such as spared upper stages and defunct spacecraft. First, the images are calibrated by applying master BIAS, DARK and FLAT FIELD images. Then the AIJ is used to extract brightness of an object from the calibrated frames. This product, a light curve, is then analyzed by using FMPI's internal Matlab script *LCProcessing.m* which uses Phase-Dispersion Minimization (PDM) method [13] to extract the apparent rotation period, phase-diagram and amplitude. Obtained data is stored in the FMPI's light curve public catalogue [10] or are further processed for color photometry [14] or attitude estimation [15]. The GUI of *LCProcessing.m* script can be seen in Fig. 5. Plotted is the light curve of Gorizont 7 (83066A) observed by AGO70 night of August 17th 2017. The PDM method determined the apparent rotation period to be 38.4 s $\pm 0.03 s$.

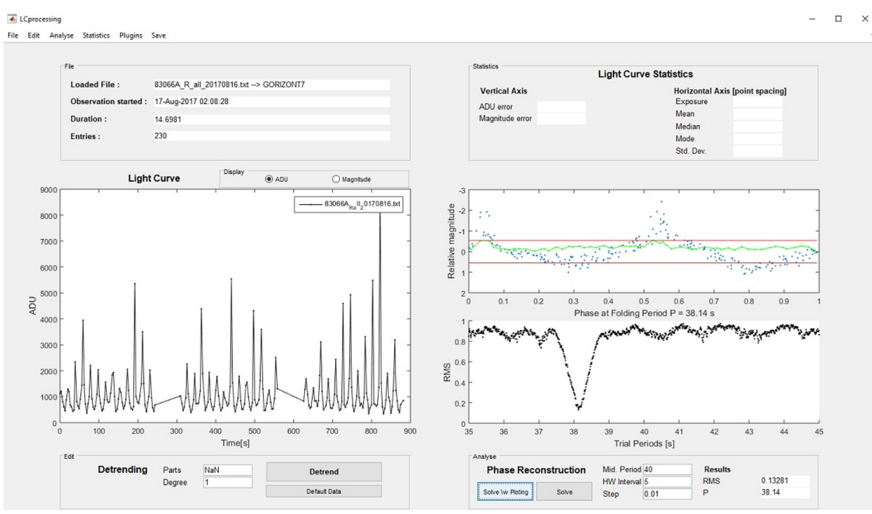

Fig. 5: Main GUI components of the FMPI's matlab script *LCProcessing.m* used for the time series analysis and phase diagram construction.

3.3 FMPI's Image Processing System

There are currently many well-known image processing systems being employed all over the world for scientific observations of space debris and Near Earth Asteroids, e.g., Apex II [16] and MOPS Pan-STARRS [17]. Inspired by the aforementioned state of the art systems, we developed our own image processing pipeline. The Image Processing System (IPS) is a tool for image processing based on own and freely available algorithms and libraries [8]. The advantage of IPS when compared to the previously two mentioned tools, Astrometrica and AIJ, is its applicability for series containing streak-like features which are common for space debris observations (see Fig. 3 and Fig. 4). At this moment IPS consists of 9 IPEs: image reduction, background estimation, objects search and centroiding, star field identification, astrometric reduction, masking/screening, tracklet building, object identification and data format transformation. The pipeline is robust enough to process raw FITS images into tracklets, which are then converted into internationally established data formats e.g. CCSDS TDM [18] or Minor Planet Center (MPC) formats. For more infromation about IPS, please, refer to [8] and [19].

3.4 TLE improvement

Once the astrometric data are acquired for object, they can be used to improve the TLEs. This should lead to improvement of the tracking direction of SLR system and in increase of its efficiency. In current project we are cooperating with two international partners which operate their own SLR stations. The ZIMLAT system of the Astronomical Institute of the University Bern, Switzerland is a hybrid system capable to perform passive and also active optical measurements. The Graz SLR station is a well-established in the LEO space debris SLR tracking.

The basic logic behind the TLE improvement to be performed by AGO70 system and be provided to the SLR stations is plotted in Fig. 6. Once the FITS images are acquired by the AGO70 system, they will be send to the IPS system. This system performs segmentation and astrometric reduction and extract the astrometric measurements of the LEO object. Then this data are provided to the TLE improvement S/W which will modify the TLE data, TLE data used for the pointing determination, by iteratively alternating some of the TLE parameters, e.g., reference epoch or mean motion, until the smallest residuals between observed and calculated (O-C) positions are reached. Then this data is sent to the SLR stations which use it for the accurate pointing. The TLE improvement S/W is under development at this moment.

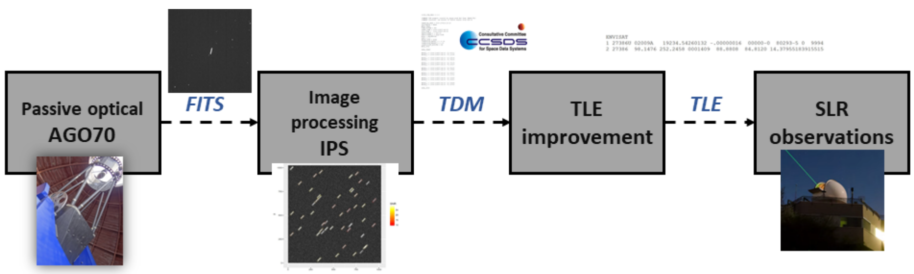

Fig. 6: General scheme demonstrating the chain for LEO tracking improvement starting with passive optical measurements, continuing with the image processing and TLE improvement and finalizing with SLR measurements to LEO object.

4. RESULTS

This section presents results obtained for the first validation of the IPS system which was performed on the astrometric data acquired for GPS/GLONASS and LEO satellites and on the photometric data acquired of GEO upper stage. For the IPS validation we were focusing at this stage on the features like successful segmentation and object recognition, astrometric reduction, tracklet building and output data quality.

4.1 Astrometry of GNSS

The detailed analysis of the system astrometric accuracy and identification of the epoch bias is presented in the work [10]. In this section we compared the astrometric data acquired by the Astrometrica tool and data processed by IPS. FITS images were acquired by using sidereal tracking (see Fig. 3a). In total, we processed ten series for 9 individual objects acquired during three nights, 25^{th} of February 2018, 21^{st} of March 2018 and 3^{rd} of May 2018. We calculated the difference between Astrometrica and IPS positions and plotted the differences in the right ascension, declination and total difference in Fig. 7. In average, the total difference when compared to Astrometrica, is 1.1 ± 0.4 arc-sec. For the right ascension and declination it was 0.9 ± 0.3 arc-sec and 0.6 ± 0.2 arc-sec, respectively.

4.2 Astrometry of LEO

To get the first impressions on how the IPS is handling FITS images with long streaks, we processed frames for LEO objects, e.g., frames plotted also in Fig. 4a and Fig. 4b. The results can be seen Tab. 1. First, the data was extracted for

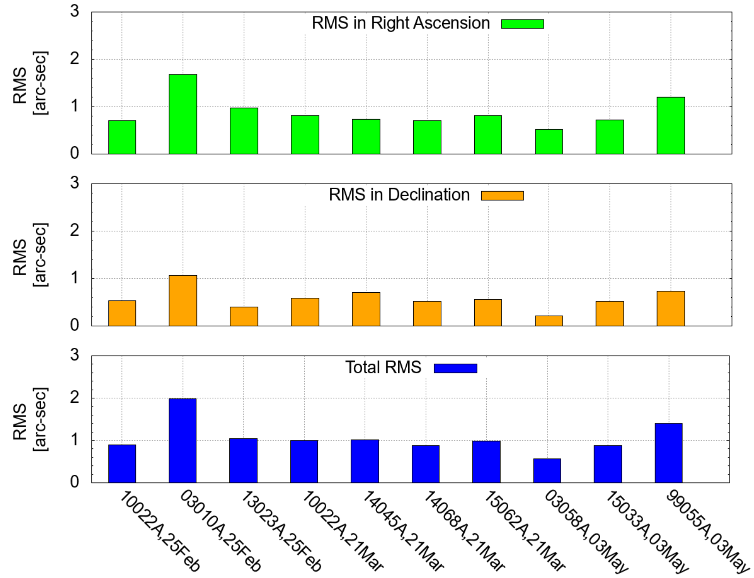

Fig. 7: RMS calculated for the right acsencion (up), declination (center) and total angular distance (down) for GNSS objects. Images have been processed by Astrometrica and IPS. Plotted is the resulting angular difference between these two solutions. Data acquired in 2018.

objects such as satellites Sentinel 3B (18039A), Ajisai (86061A), and upper stages SL-11 R/B (70089B) and SL-12 R/B(2) (02037D). We performed the centroiding on the streaks, as well as on the points. We used the identified stars to perform astrometric reduction and the obtained solution was then applied to the object's frame coordinates. This data was than compared to the calculated ephemerides obtained by using SatEph program (see section 2.1) and TLE data with reference epoch (in Tab. 1 column no. 3, 2^{nd} row) closest to the observation epoch (in Tab. 1 column no. 3, 1^{st} row). The total O-C difference is on the level between 0.41 arc-min for the SL-11 R/B up to 2.59 arc-min for the Starlink satellite. However, the values plotted in Tab. 1 should be taken cautiously. The O-C angular difference in this analysis can have different source from the TLE and SPG 's uncertainties, through the SatEph calculations up to the measurement data errors acquired by the IPS. For a more accurate analysis we will use in the future the so-called Consolidated Prediction Format (CPF) files generated by the GNSS and SLR communities which can then be used as a ground-truth data for the comparison.

4.3 Photometry of MEO and GEO

The IPS should be used for the semi-automated processing of light curves acquired by AGO70 system. To investigate its applicability on the long series with GEO tracking, we processed several different observations. An example of the photometric series processed by the IPS can be seen in Fig. 8, where we plotted a light curve of object Delta 4 R/B (02051B). There are three types of information plotted in Fig. 8: measurement points extracted by using AIJ [ADU]; measurement points extracted by using IPS [ADU]; and their difference [ADU]. This is the same series as plotted in Fig. 3b.

While the measurements plotted in Fig. 3b for AIJ have been acquired by using circular aperture with radius of 6 pixels, for the IPS we used squared aperture with side of 10.6 pixels to get the same size for the investigated area of around 113.1 pixels. The total RMS between AIJ and IPS obtained data points was 181.5 ADU, where in general, higher signal was extracted for the object by using the IPS than AIJ.

5. CONCLUSIONS

We presented our 70-cm Newtonian telescope dedicated to the space debris observations. This system has currently limited tracking capabilities and thanks to the modifications to the observation strategies is able to observe objects

Table 1: Observed data (AGO70) minus calculated data (TLE/SGP4) (O-C) for LEO objects observed by the AGO70 system in August 2019. The listed observation times are for the middle of exposure. *FITS frame was acquired by using the object tracking.

COSPAR	Name	t_{obs} t_{TLE} [UTC]	RA_{IPS} [deg]	DE_{IPS} [deg]	RA_{TLE} [deg]	DE_{TLE} [deg]	Δ_{RA} [arc-min]	Δ_{DE} [arc-min]	Δ_{Total} [arc-min]
18039A	Sentinel 3B	2019-08-11 19:21:00.05 2019-08-10 19:33:21.71	336.56375	29.86569	336.58271	29.88485	0.99	1.15	1.51
86061A	Ajisai	2019-08-12 02:40:00.05 2019-08-10 18:02:56.06	321.58906	45.42585	321.57158	45.41245	0.74	-0.80	1.09
02035D	SL-12 R/B(2)*	2019-08-27 19:55:24.57 2019-08-26 18:10:17.31	266.86760	6.45256	266.88354	6.44291	0.95	-0.58	1.11
70089B	SL-11 R/B	2019-08-09 19:09:00.05 2019-08-08 13:12:42.86	250.45227	13.55900	250.45473	13.56548	0.14	0.39	0.41
19029B	Starlink OBJ B	2019-08-08 19:20:00.10 2019-08-07 07:53:18.03	180.89637	51.22382	180.89009	51.18078	0.24	-2.58	2.59

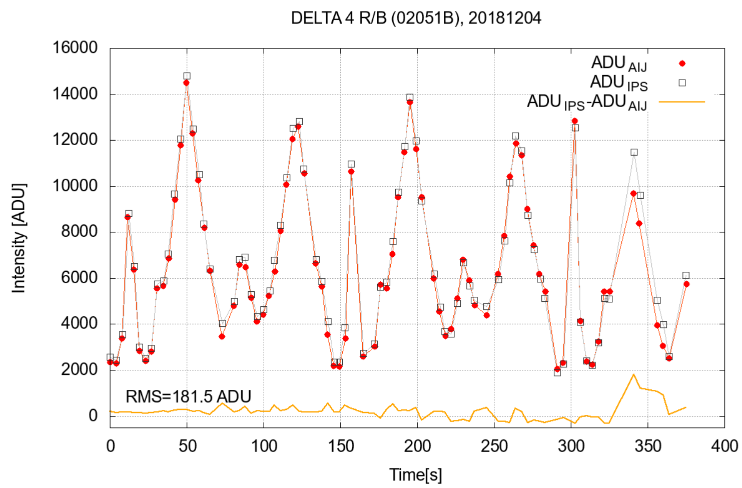

Fig. 8: Light curve of object 02051B (DELTA 4 R/B) observed by AGO70 during the night 4^{th} of December 2018 by using 1.0 s exposure and R filter. Data processed by AstroImageJ (red filled dots) and by IPS (black empty squares). The total RMS between these two data sets was 181.5 ADU.

on from low-earth orbits up to geosynchronous orbits. For GEO and highly eccentric orbits we turn off the sidereal tracking which results to GEO tracking during observations. For GPS orbits we use very short exposure times to acquire point-like features for satellites, as well as for the stars. For LEO objects two strategies are exploited. First, the observations are acquired when the sidereal tracking is used and the object appears as a streak and stars as points. Second, the telescope control unit is set for short period of time of the tracking velocities of the object and the object appears as a point and stars as streaks. Timing for such data acquisition needs to be accurate, in our case it is up to 80 ms and it proved to be sufficient.

In our work we applied by us developed Image Processing System (IPS) to the astrometric series acquired for the GPS satellites and LEO objects and to the photometric series acquired for the upper stage on highly eccentric orbit. Processing is working properly concerning the segmentation, astrometric reduction and tracklet building. To evaluate the quality of the extracted data, namely astrometric positions and photometric light curves, we compared obtained data to the reference data extracted by using conventional image processing tools Astrometrica and AstroImageJ, respectively. In the case of LEO objects, we compared the extracted positions to the ephemerides calculated by our internal planing tool SatEph which uses available Two Lines Elements data and SGP4 model. The performed initial analysis has shown that the difference between IPS and Astrometrica results for the GPS satellites is on the level of 1.1 ± 0.4 arc-sec. For LEO objects we got difference fully dependent on the object and its TLE, from 0.41 arc-min to 2.59 arc-min. For the photometry and light curve construction we compared the results for one light curve extracted by the IPS and simultaneously by the IAJ. The resulting difference between those two data sets was on the level of RMS = 181.5 ADU.

Our future work will focus on more accurate data quality analysis of the image processing. For GPS satellites and LEO objects we will use the so-called Consolidated Prediction Format (CPF) files generated by the GNSS and SLR communities which can then be used as a ground-truth data for comparison with our measured IPS data. The next step for the light curve analysis is to compare series generated by AIJ and IPS by using our own tools for the light curve processing which provide output in the form of a phase curve and its fit along with the error estimates. The error estimated for AIJ and IPS will be used to qualitative comparison of those two approaches. The mount control system will be developed which will allow us to perform follow-up observations of LEO objects for more than just few seconds. Last, but not least, the S/W for the TLE improvement will be developed to support the SLR stations for space debris tracking.

ACKNOWLEDGMENTS

The presented work was performed under a programme of ESA PECS activity "ImpEuroLEOTrack: Improvement of European capabilities for LEO objects tracking with optical passive sensors", ESA Contract no. 4000126272/18/NL/NDe.

6. REFERENCES

[1] B. Bastida Virgili, J.C. Dolado, H.G. Lewis, J. Radtke, H. Krag, B. Revelin, C. Cazaux, C. Colombo, R. Crowther, and M. Metz. Risk to space sustainability from large constellations of satellites. *Acta Astronautica*, 126:154 – 162, 2016. Space Flight Safety.

[2] H. Lewis, J. Radtke, A. Rossi, J. Beck, M. Oswald, P. Anderson ans B. B. Virgili, and H. Krag. Sensitivity of the space debris environment to large constellations and small satellites. *Proceedings of the 7th European Conference on Space Debris, Darmstadt, Germany*, 2017.

[3] M. Shappirio, J.F. McGarry, J. Bufton, J.W. Cheek, D.B. Coyle, S.M. Hull, P.R. Stysley, X. Sun, R.P. Young, and T. Zagwodzki. Application of satellite laser ranging techniques for space situational awareness efforts. *Proceedings of Advanced Maui Optical and Space Surveillance Technologies Cenference (AMOS), Conference 2016, Maui, Hawaii, USA*, 2016.

[4] Georg Kirchner, Franz Koidl, Fabian Friederich, Ivo Buske, Uwe Volker, and Wolfgang Riede. Laser measurements to space debris from graz slr station. *Advances in Space Research*, 51(1):21 – 24, 2013.

[5] Z. Zhang, H. Zhang, M.L. Long, H. Deng, Z. Wu, and W. Meng. High precision space debris laser ranging with 4.2 w double-pulse picosecond laser at 1 khz in 532nm. *Optik*, 179:691 – 699, 2019.

[6] A. Milani, D. Farnocchia, L. Dimare, A. Rossi, and F. Bernardi. Innovative observing strategy and orbit determination for low earth orbit space debris. *Planetary and Space Science*, 62(1):10 – 22, 2012.

[7] USSTRATCOM. Space-track.org.

[8] J. Silha, S. Krajcovic, D. Zilkova, J. Vilagi, F. Duris, J. Toth, M. Trujillo, Flohrer, and V. Nagy. Slovak optical telescope and image processing pipeline for the space debris and nea observations and research. Proceedings of the 7th European Conference on Space Debris in Darmstadt, 2019.

[9] D. A. Vallado, P. Crawford, R. Hujsak, and T. S. Kelso. Revisiting spacetrack report 3. *The AIAAAAS Astrodynamics Specialist Conference, American Institute of Aeronautics and Astronautics*, pages 1–88, 2006.

[10] J. Silha, S. Krajcovic, J. Toth, M. Zigo, L. Novak, D. Zilkova, J. Vilagi, P. Zigo, L. Kornos, J. Simon, T. Schildknecht, E. Cordelli, A. Vananti, H. Mann, A. Rachman, and Ch. Paccola. Space debris observations with the Slovak AGO70 telescope: astrometry and light curves (under revision). *Advances in Space Research*, 2019.

[11] H. Raab. Astrometrica tool, www.astrometrica.at. 2016.

[12] Karen A Collins, John F Kielkopf, Keivan G Stassun, and Frederic V Hessman. Astroimagej: image processing and photometric extraction for ultra-precise astronomical light curves. *The Astronomical Journal*, 153(2):77, 2017.

[13] R. F. Stellingwerf. Period determination using phase dispersion minimization. *The Astrophysical Journal*, 224:953–960, 1978.

[14] M. Zigo, J. Silha, and S. Krajcovic. BVRI photometry to space debris objects at the Astronomical and geophysical observatory in Modra. *Proceedings of Advanced Maui Optical and Space Surveillance Technologies Cenference (AMOS), Conference, Maui, Hawaii, USA*, 2019.

[15] V. Williams. Location of the rotation axis of a tumbling cylindrical earth satellite by using visual observations: Part i: Theory. *Planetary and Space Science*, 27(6):885 – 890, 1979.

[16] V. Kouprianov. Distinguishing features of ccd astrometry of faint geo objects. *Advances in Space Research*, 41(7):1029 – 1038, 2008.

[17] P. Veres, R. Jedicke, L. Denneau, R. Wainscoat, M. J. Holman, and H.-W. Lin. Improved asteroid astrometry and photometry with trail fitting. *Publications of the Astronomical Society of the Pacific*, 124, 09 2012.

[18] The Consultative Committee for Space Data Systems. Tracking data message. *CCSDS 503.0-B-1, Blue Book, November 2007*, 2017.

[19] J. Silha, S. Krajcovic, J. Toth, L. Kornos, J. Vilagi, P. Zigo, J. Simon, D. Kalmancok, M. Hamara, D. Zilkova, L. Novak, M. Zigo, F. Duris, V. Nagy, R. Durikovic, T. Schildknecht, E. Cordelli, A. Vananti, Ch. Paccolat, A. Rachman, J.K. Mann, M. Trujillo, and T. Flohrer. Slovakian optical sensor for HAMR objects cataloguing and research. Proceedings of 69th Internatonal Astronautical Conference in Bremen, 2018.